# Adsorption, Kinetic and Thermodynamic Studies of Copper(II) Removal by Modified Activated Carbon derived from Sugarcane Bagasse (MSCB)

**Singh I.[1], Srivastava A.[2*], Nayak R.[3], Pandey P.K.[1] and Naik R.M.[1*]**
1. Department of Chemistry, University of Lucknow, Lucknow-226007, U.P., INDIA
2. Department of Chemistry, GLA University, Mathura-281006, U.P., INDIA
3. Deen Dayal Upadhyay Gorakhpur University, Gorakhpur-273009, U.P., INDIA
*aabhichem@gla.ac.in; naik_rm@rediffmail.com

## *Abstract*

*Over the past few years, environmental concerns regarding heavy metal contamination have grown. Removing Cu(II) from wastewater from industry is crucial for environmental sustainability. Sugarcane bagasse, an agricultural byproduct, is widely available in many countries. Its fibrous texture and high cellulose, hemicellulose and lignin content make it ideal for heavy metal adsorption. By phosphoric acid activation, sugarcane bagasse (SCB) was converted into low-cost activated carbon and grafted with EDTA to make modified sugarcane bagasse (MSCB). Its ability to adsorb Cu(II) ions from aquatic solutions was investigated.*

*A porous framework with 2073 $m^2/g$ surface area was discovered in the MSCB using SEM, BET and FTIR investigations. The adsorption system adhered to a pseudo-second-order kinetic model, with the equilibrium time being determined at 230 minutes. The Langmuir model accurately simulated the adsorption isotherms. A mechanism involving ion exchange was suggested by the substantial pH dependence of Cu(II) adsorption on MSCB. Investigations on regeneration revealed that MSCB could be reused multiple times through desorption using HCl.*

**Keywords:** Copper, Modified sugarcane bagasse, Langmuir adsorption isotherm, Kinetic modeling, pH, Equilibrium time.

## Introduction

Numerous techniques for eliminating heavy metals from waste water have garnered increased attention from researchers in the past few decades. Heavy metal contamination in water causes serious health problems as well as damage of the environment[19,25,29]. Therefore, the presence of non-degradable, hazardous and toxic heavy metal ions in industrial effluent has been very harmful to aquatic and human life[26,28]. The main contributor of wastewater containing heavy metal ions is the industrial sector like the mining industries, metal plating, electroplating, fertilizer formation, pesticide synthesis, batteries and textile industries[15,17,20].

**** Author for Correspondence***

The toxicity of heavy metals attracts more attention and hence extra efforts of research are made to find out the best route for their removal. The toxicity of heavy metal ions causes damage to the kidney and nervous system, reproductive system, brain, liver, severe stomachache, hypertension, reduced blood synthesis and may also lead to miscarriage in pregnant women[7,38]. Copper is known to be one of the major pollutants released by fertilizer, paper, electroplating, roofing, plumbing, air conditioning and electric wiring industry etc.[10,11,22,37]

In the realm of heavy metal toxicity mitigation, a plethora of techniques exist to address this concern. These techniques encompass membrane separation, ion exchange, electrolysis, adsorption and chemical precipitation. Among the above-mentioned methodologies, adsorption has been empirically demonstrated to be a straightforward and highly efficient approach[21]. Activated carbon finds widespread use as an adsorbent in several applications related to wastewater treatment. The material exhibits a significantly enhanced level of porosity, showcasing a substantial internal surface area, demonstrating commendable mechanical strength[1,24,30]. Even though its extensive utilization is across various industries, activated carbon continues to be a material of considerable cost.

Hence, it becomes imperative to conduct an in-depth exploration and advancement of cost-efficient carbon materials that can be effectively utilized for the purpose of mitigating water pollution. A diverse range of cost-effective materials has been employed for the purpose of extracting impurities from aquatic solutions. These materials encompass algal wastes, pecan shells, palm shells, peanut hulls, coconut shells and hazelnut husks[3,9,12,16,34,42]. Many researchers are interested in this low-cost adsorption approach because it does not require a sophisticated regeneration methodology.

This study evaluates the effectiveness of modified sugarcane bagasse (MSCB) in removing Cu(II) ions from wastewater. The presence of functional groups such as =C-O-, –C=O, -NH and OH on MSCB facilitates the biosorption of heavy metal ions from aqueous solutions[32,39]. The investigation of MSCB properties involves the utilization of numerous analytical techniques including FTIR, BET and SEM. The investigation encompassed an examination of the impact of different operating parameters including contact time, initial [Cu(II)], adsorbent dose, temperature and pH of the solution.

The investigation focused on studying adsorption isotherms, employing various adsorption models such as the Langmuir and Freundlich.

Furthermore, kinetic models, specifically pseudo-second-order and pseudo-first-order, were utilized to analyze the experimental findings, thereby deepening our comprehension of the adsorption dynamics of Cu(II) ions onto MSCB. Thermodynamic investigations were also conducted to ascertain the nature of the adsorption phenomenon (endothermic or exothermic).

## Material and Methods

All experiments were conducted using double-deionized water (DDW) and analytical-grade reagents over the entire study. Copper nitrate (AR, Fisher Scientific, India) and EDTA (AR, Fisher Scientific, India) utilized were of utmost purity. A supply solution of 1000 mg/L of $Cu(NO_3)_2$ was meticulously made with double distilled water (DDW). Himedia India supplied $H_3PO_4$ (99.9 %) which was utilized without subsequent purification. NaOH (Fisher Scientific, India) and HCl (Merck, India) solutions were employed to modulate the pH employing a Systronics 361 pH meter. FT-IR spectrophotometer (IR Affinity, Shimadzu) was utilized to examine the functional groups in MSCB. Utilizing a Scanning electron microscope (S4800, Hitachi, Japan), MSCB's surface morphology was observed.

**Preparation of MSCB:** The sugarcane bagasse (SCB) was collected from local areas around Lucknow (India). SCB was crushed, washed thoroughly with DDW to eliminate impurities and dried in an oven for 6-8 hours at 100 °C. After drying, the residue was ground and sieved to obtain the sugarcane bagasse powder (SCBP) of the desired particle size (100 µm). SCBP (10 g) reacted with 1.5 M phosphoric acid (100 mL) in a round bottom flask at 100 ± 2 °C in contact for 1 hour. Afterward, the SCBP was extensively rinsed with DDW until the pH of the filtrate reached a neutral level.

Acid treatment was done to improve the sorption capacity and porosity of the adsorbent[36,43]. For grafting, 10 g of SCBP adsorbent was added to 50 ml of ethylene diamine tetra-acetic acid (EDTA) at a temperature of 100 ± 2 °C. The mixture was constantly stirred for one hour. The MSCB underwent a drying process at a temperature of 80 °C for 12 hours. Subsequently, the MSCB was ground to acquire particles 100 µm size and later kept in a desiccator for future utilization.

**MSCB Adsorption Experiments:** Adsorption experiments using MSCB were conducted to discover the optimal conditions for the Cu(II) adsorption on MSCB. For that, calculated amount of MSCB and 50 ml of Cu(II) solution (20 mg/L) were carefully introduced into a 500 ml beaker. NaOH or HCl solution was used to maintain the pH of the reacting mixture prior to the addition of the adsorbent. The test solutions were then shaken for 300 minutes at 150 rpm in a thermostat rotator while maintaining a consistent temperature of 303 K.

Subsequently, the supernatant solutions underwent filtration and the quantification of metal content in each flask was accomplished utilizing a PerkinElmer 900 series atomic absorption spectrophotometer. The uptake of Cu(II) at equilibrium, $q_e$ (mg/g) and the % removal of Cu(II), was determined using equation 1 and 2.

$$q_e = \frac{(C_o - C_e) \times V}{m} \quad (1)$$

$$\text{Percentage Removal} = \frac{(C_o - C_e) \times V \times 100}{C_o} \quad (2)$$

The initial concentration of Cu(II) ions ($C_o$), equilibrium concentration ($C_e$), adsorbent mass (m) and solution volume (V) are the variables.

**Desorption Studies:** The MSCB that had been synthesized was exposed to Cu(II) (20 mg/L) until it reached a state of equilibrium. The equilibrium concentration of adsorbate, $C_{ad}$ (mg/L), was determined by subtracting the starting concentration ($C_o$) from the equilibrium concentration ($C_e$). Subsequently, the exhausted MSCB was isolated from the solution and rinsed with DDW to eliminate any unadsorbed Cu(II) ions. Following the drying process at 40 °C within a vacuum oven, the sample was agitated for desorption experiments using DDW, 0.1 N NaOH and HCl in that order. Following desorption, measurements were made of the Cu(II) concentrations (mg/L) that desorbed $C_{de}$. The following formula was used to get the percentage of desorption:

$$\% \text{ Desorption} = \frac{C_{ad}}{C_{de}} \times 100 \quad (3)$$

## Results and Discussion

**Characterization of MSCB:** Figure 1a demonstrates the SEM image of MSCB powder prior to adsorption. The image exhibits an asymmetric, rough and porous structure. Furthermore, the presence of micro-sized active sites or cavities suggests that MSCB powder possesses significant potential as an adsorbent for the efficient capture of Cu(II) ions. The surface area of adsorbents stands out as one of their most crucial attributes. Figure 1b represents the nitrogen adsorption-desorption isotherms for prepared MSCB. It was found that MSCB exhibited a surface area of 2073 $m^2/g$ which is notably substantial for the efficient adsorption of Cu(II). The average pore diameter of 7.3 nm suggests the mesoporous structure of MSCB[5].

The FT-IR spectra of MSCB were obtained employing the KBr pellet approach, covering the wavenumber range of 4000-400 $cm^{-1}$. The FT-IR spectra of MSCB are shown in figure 2. The FTIR spectra of MSCB revealed that the absorbance bands had peaks at 3412, 2870, 1680, 1590, 1300 and 1100 $cm^{-1}$. Other researchers have documented the majority of these bands for various carbon compounds. A

band within the range of 3500-3300 cm-1 is attributed to -OH and/or N-H stretching vibrations[23]. A peak between 3000-2875 $cm^{-1}$ is indicative of alkane C-H stretching. At 1680 $cm^{-1}$, we observe the distinctive C=O stretching of the carboxylic acid group[31]. Peaks at 1590 and 1300 $cm^{-1}$ are indicative of $sp^2$-hybrid carbon-carbon (C=C, stretching) and $sp^3$-hybrid C-H bending respectively[35].

A peak observed at 1100 $cm^{-1}$ signifies the occurrence of C-O stretching; however, peaks below 1000 $cm^{-1}$ are caused by distinct functional groups' bending vibrations. The presence of the –OH and $NH_2$ groups indicates that there has been a significant amount of interaction between the adsorbate and the adsorbent, which could help Cu(II) ions to adsorb onto the MSCB 's active sites.

**Influence of pH on Cu(II) removal:** The primary variable influencing adsorption efficacy is pH because it influences the interface properties of the adsorbate and adsorbent by altering the surface charge, the behavior of the adsorbate ions in reaction mixture and deprotonation/protonation of the distinct functional groups on the adsorbent surface. To avert the precipitation of Cu(II) and enhance removal efficiency, an adsorption study was conducted across a pH spectrum of 1.5 to 8 as illustrated in figure 3a.

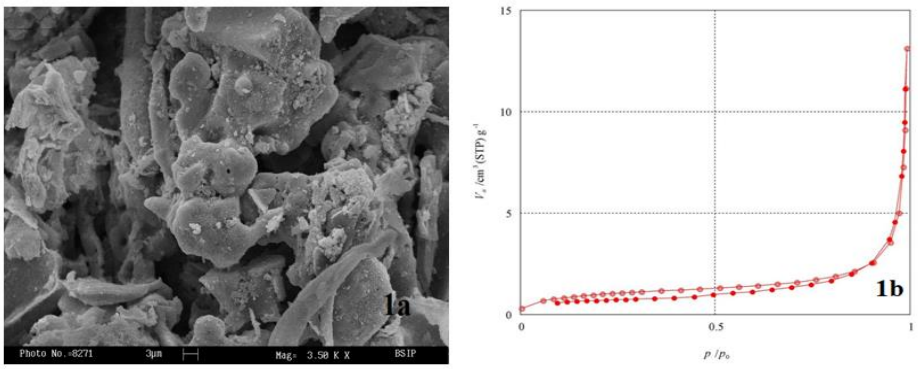


**Figure 1: (a) SEM images of MGNS, (b) Nitrogen adsorption-desorption isotherms for prepared MSCB**

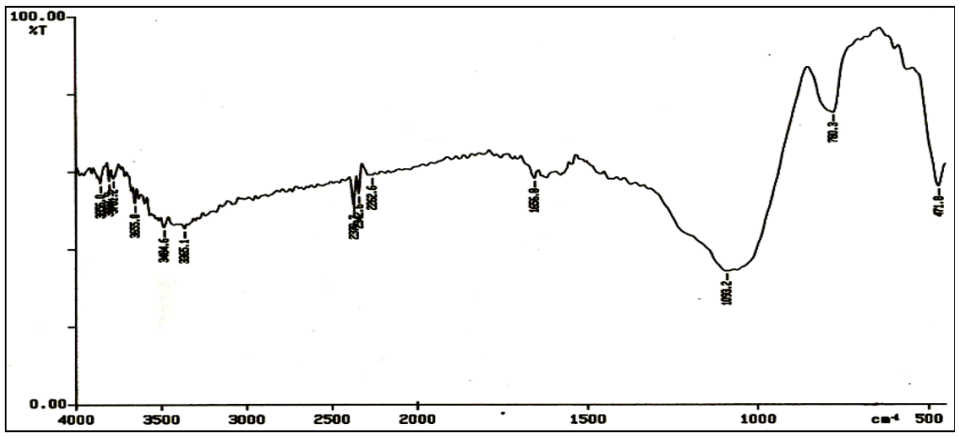


**Figure 2: FT-IR Spectra of MGNS**

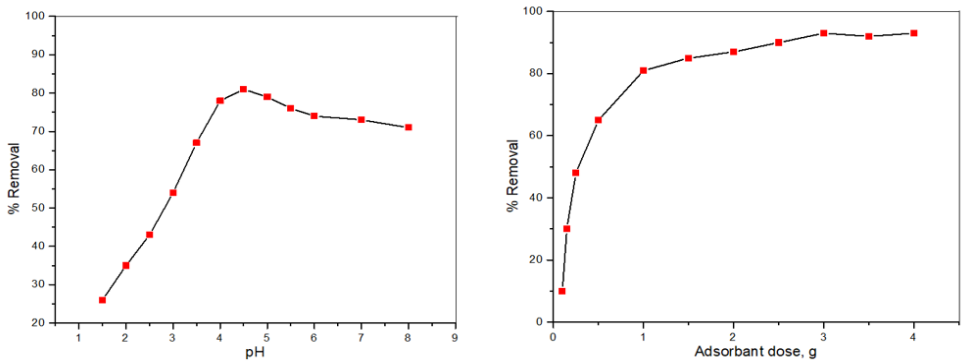


**Figure 3: (a) Influence of pH on % removal of Cu(II) at Contact time = 230 min, Temperature = 303 K, MSCB dose = 1.0 g/L and [Cu(II)] = 20 mg/L, (b) Influence of MSCB dose on % removal of Cu(II) at contact time = 230 min, Temperature = 303 K, MSCB dose = 1.0 g/L, pH = 4.5 ± 0.1 and [Cu(II)] = 20 mg/L**

Cu(II) adsorption by MSCB was extremely pH sensitive; when the pH level rose from 1.5 to 4.5, the removal efficacy increased rapidly from 26.5% to 81.2%. $H_3O^+$ and Cu(II) competing for adsorption sites on MSCB provide an explanation for the results. There may be less adsorbed Cu(II) at low pH levels due to competition between Cu(II) and extra $H_3O^+$. The covered $H_3O^+$ leaves the MSCB surface when the pH rises, making the sites accessible to Cu(II)[44].

Furthermore, as pH rises, the amine and oxygen-bearing functional groups on the MSCB surface deprotonate, increasing the negative charge on the MSCB surface[2]. As a result, Cu(II) adsorption increased due to the increased electrostatic attraction between MNGS and Cu(II). Surprisingly, with further change in pH values from 5.5 to 8.0, no considerable changes have been observed in % removal of Cu(II) ions. Therefore, the subsequent experiments have been performed at pH 4.5.

**Influence of MSCB dose on Cu(II) removal:** The amount of adsorbent utilized is one of the most crucial variables that affects how well the adsorption process goes. Removal effectiveness usually increases with an increase in the adsorbent dosage. At considerably greater adsorbent dosages, however, there was no discernible difference in removal efficiency. The MSCB dose was adjusted between 0.1 and 4.0 g/L in order to discover the optimal adsorbent value for Cu(II) removal. The elimination of Cu(II) ions improves from 10.4% to 93.2% when the MSCB dose is raised from 0.1 to 3.0 g/L (Figure 3b). With increase in adsorbrnt doses, the adsorbent's large surface area and more active adsorbing sites (more availability of functional groups) are responsible for the increase in adsorption effectiveness. Higher doses of the adsorbent, however, cause the active adsorbing sites to agglomerate and overlap, reducing surface area and active adsorbing sites maintaining a constant adsorption capacity[8,27].

**Study of variation of contact time:** Adsorption, a time-dependent phenomenon, is critical in the design of innovative adsorption systems. The temporal interplay between metal ions and adsorbents facilitates the elucidation of the kinetic propensity for binding and sequestration of metal ions, alongside the identification of the optimal time range for achieving maximal removal efficiency. The observed trend in the % elimination of Cu(II) ions as an indicator of contact time is depicted in figure 4a.

Initially, it has been observed that the adsorption rate exhibits a rapid increase during the initial 110 minutes. Subsequently, the rate experiences a gradual increase until reaching 230 minutes, at which point it stabilizes, indicating the attainment of adsorption equilibrium. The initial swift adsorption can be attributed to the robust affinity between the Cu(II) ions and the MSCB 's active sites[13,33]. As the procedure advanced, the rate of adsorption reduced because the active sites of MSCB were gradually being occupied. The saturation of the MSCB 's active sites is what causes the consistency in the adsorption rate.

**Study of variation of copper(II) ions solution concentration:** The starting metal ion concentration plays a crucial role in establishing the adsorption rate for effective adsorption. The eliminated percentage of Cu(II) declines from 81.0 % to 30.5 % as the [Cu(II)] rises from 5 mg/L to 100 mg/L. (Figure 4b). The constancy of the MSCB dosage resulted in a limitation on the total number of available active sites of MSCB, thereby diminishing the effectiveness of Cu(II) removal.

**Adsorption Isotherms:** In order to investigate the adsorption phenomena and the underlying mechanisms at play, the adsorption isotherm models of Freundlich and Langmuir were employed to analyze the Cu(II) adsorption results on MSCB. At equilibrium, the Langmuir adsorption equation for a monolayer of adsorbate adsorbed onto the adsorbent surface with finite active sites can be expressed as[18]:

$$\frac{C_e}{q_e} = \frac{1}{q_{max} K_L} + \frac{C_e}{q_{max}} \quad (4)$$

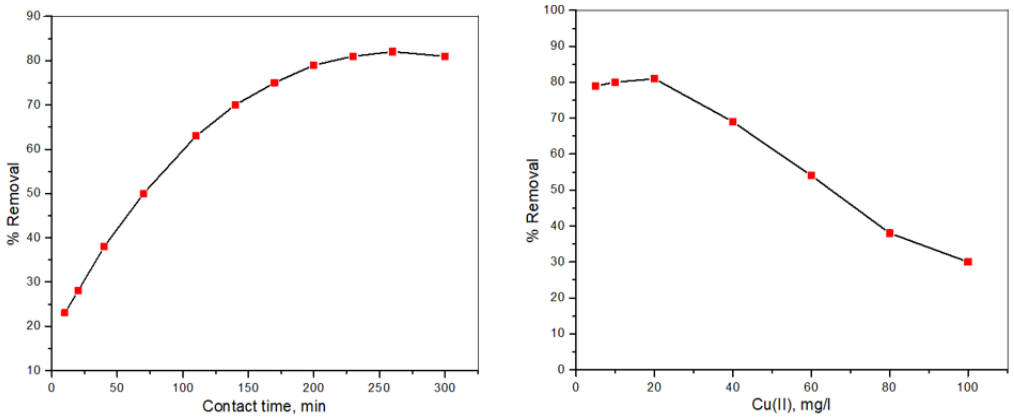


**Figure 4: (a) Influence of contact time on % elimination of Cu(II) at MSCB dose = 1.0 g/L, pH = 4.5 ± 0.1, Temperature = 303 K and [Cu(II)] = 20 mg/L, (b) Influence of [Cu(II)] on % removal of Cu(II) at Contact time = 230 min, MSCB dose = 1.0 g/L, pH = 4.5 ± 0.1 and Temperature = 303 K**

where Langmuir constant is $K_L$ (L/mg), the monolayer adsorbate adsorption performance or capacity is $q_{max}$ (mg/g); the amount of Cu(II) ions adsorbed on MSCB at equilibrium is indicated by qe (mg/g), while the Cu(II) equilibrium concentration is $C_e$ (mg/L).

Langmuir constant is associated with the free energy of adsorption. Figure 5a illustrates a graph correlating $C_e$ and $C_e/q_e$, demonstrating a linear relationship. The $q_{max}$ and $K_L$ values may be ascertained by analyzing the slope (1/ $q_{max}$) and intercept (1/ $q_{max}$ $K_L$) of the graph. These values are recorded in table 1. The linearity observed in the plot depicted in figure 5a serves as evidence supporting the validity of the Langmuir model. The outcomes of our investigation's calculation of the monolayer adsorption performance or capacity are superior to those of the previously published work. Table 2 provides a comparison of the current work's monolayer adsorption capacity values with those found in the literature.

The subsequent equation serves to delineate a dimensionless equilibrium parameter $R_L$, which is employed to evaluate the favorability of adsorption:

$$R_L = \frac{1}{1 + K_L C_o} \quad (5)$$

where the initial [Cu(II)] is $C_o$ (mg/L) and Langmuir constant is $K_L$ (L/mg). The isotherm type can be classified as irreversible unfavorable ($R_L > 1$), ($R_L = 0$), linear ($R_L = 1$), or favorable ($0 < R_L < 1$) based on the $R_L$ value[4].

The Freundlich model is suited to highly heterogeneous surfaces and multi-layer adsorption with no plateau. Equation 6 provides the formula for the Freundlich adsorption isotherm[14]:

$$\log q_e = \log K_F + \frac{1}{n} \log C_e \quad (6)$$

In this context, $K_F$ and n are the constants associated with the Freundlich isotherm. The linear aspect of the plot between $C_e$ and $\ln q_e$ is illustrated in figure 5b. Table 1 presents the values of KF and n, derived utilizing slope (1/n) and the intercept (ln $K_F$) of the plotted data. The value of n signifies the degree of favorability regarding adsorption. A typical Langmuir isotherm is observed when the value of 1/n is less than 1.

The process of Cu(II) adsorption onto MSCB demonstrated remarkable alignment with the Langmuir isotherm model, as indicated by the impressive $R^2$ value of 0.9984. The result can be ascribed to the consistent distribution of active sites throughout the MSCB surface. Moreover, the observed $R_L$ values for the Langmuir isotherm fell within the range of 0 to 1, while the Freundlich constant 1/n exhibited a value less than 1, thereby suggesting a process that is thermodynamically favorable.

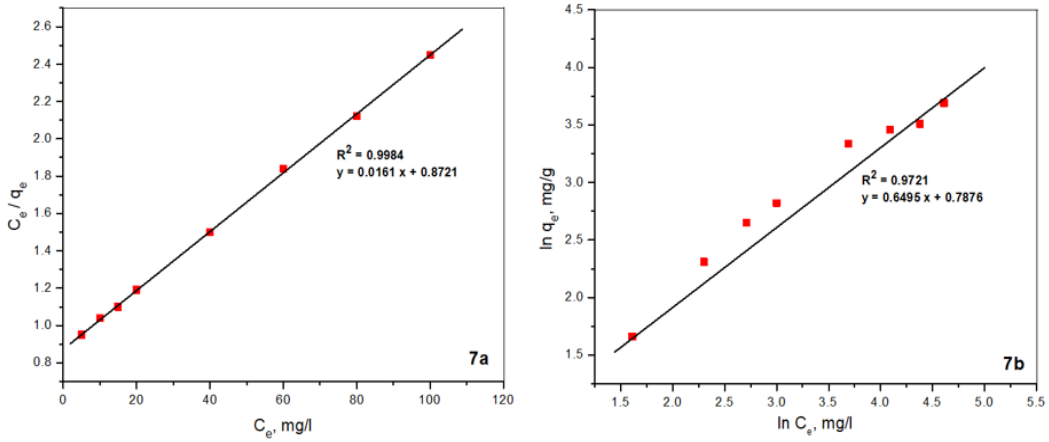


**Figure 5: (a) Plot of Langmuir isotherm model for the Cu(II) adsorption on MSCB, (b) Plot of Freundlich isotherm model for the Cu(II) adsorption on MSCB**

**Table 1**
**Freundlich and Langmuir isotherm constants for the Cu(II) adsorption onto MSCB**

| Isotherm | Constant Values |
|---|---|
| Freundlich | $K_F$ (mg/g) = 6.13 |
| | 1/n = 0.6495 |
| | $R^2$ = 0.9721 |
| Langmuir | $q_{max}$ (mg/g) = 62.11 |
| | $K_L$ (l/mg) = 0.019 |
| | $R^2$ = 0.9984 |
| | $R_L$ = 0.213 |

Table 2 presents a comparative analysis of the adsorption efficacy for Cu(II) in relation to various activated carbons derived from solid waste materials. The notable adsorption capacity demonstrated by this study highlights the promising application of MSCB as an effective adsorbent for the removal of Cu(II).

**Adsorption Kinetics:** The kinetic investigation for Cu(II) adsorption onto MSCB has been done utilizing first-order model (Lagergren's) and second-order kinetic model (Ho-McKay's). Pseudo-first-order (PFO) model, which is often provided by equation 7, is dependent on the solid adsorbent capacity[6]:

$$\log(q_e - q_t) = \log q_e - \frac{k_1}{2.303} t \quad (7)$$

Here, $q_t$ (mg/g) represents the quantity of Cu(II) adsorbed on MSCB at various time intervals whereas $k_1$ ($min^{-1}$) signifies the adsorption rate constant. Figure 6a displays a graph between $\log(q_e - q_t)$ vs time (t), which has been used to compute the values of the adsorption rate constant ($k_1$).

Table 3 provides a summary of every parameter that was computed with this model. Based on the lower values of the regression coefficient (adj. $R^2$), it appears that this model is not providing the best fit and may not be suitable for the current conditions. Based on equilibrium adsorption, the pseudo-second-order (PSO) model has been presented as[41]:

$$\frac{t}{q_t} = \frac{1}{k_2 q_e^2} + \frac{t}{q_e} \quad (8)$$

where $k_2$ (g/mg min), is the pseudo-second-order rate constant. Figure 6b illustrates the linear relationship between time t and $t/q_t$. The values of $q_e$ and $k_2$ can be found on this graph by using the slope and intercept respectively. Table 3 has the calculated values listed.

Upon comparing the outcomes of the regression coefficients, it is observed that $R^2$ exhibited a value of 0.9985 when considering the second-order reaction kinetics. Conversely, when considering the first-order reaction kinetics, $R^2$ displayed a value of 0.9764. The results obtained demonstrate that the adsorption kinetics of Cu(II) on MSCB adhere to the principles of second-order kinetics.

**Thermodynamic studies:** The investigation of how temperature affects experimental conditions has also been crucial. Figure 7 illustrates the influence of temperature on the percentage removal of Cu(II). The rise in temperature correlates with a notable enhancement in the adsorption of Cu(II) onto MSCB, likely due to the augmented kinetic energy involved.

**Table 2**
**Comparative analyses of the capacities for adsorption of Cu(II) onto diverse adsorbents**

| Adsorbent | $q_{max}$ (mg $g^{-1}$) |
|---|---|
| Grape bagasse activated carbon[14] | 43.47 |
| Groundnut seed cake power[27] | 3.7 |
| Date stone activated carbon[27] | 31.25 |
| Sesame seed cake powder[27] | 3.6 |
| Mango peel[23] | 46.09 |
| Cassava peel activated carbon[33] | 56.17 |
| Coconut cake Powders [27] | 3.7 |
| Banana leaves derived activated carbon[21] | 48.7 |
| This Study | 62.11 |

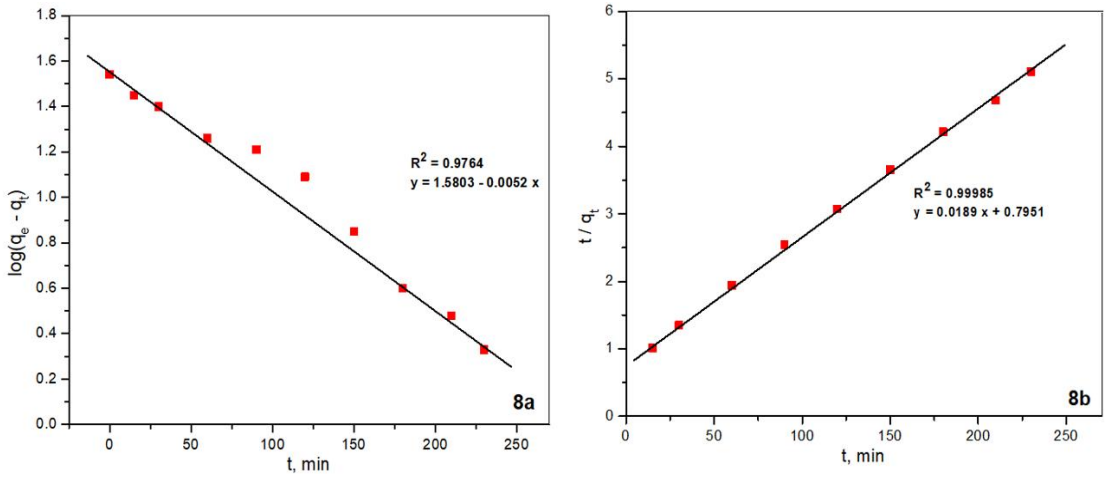


**Figure 6: (a) Pseudo-first order plot for adsorption of Cu(II) on MSCB, (b) Pseudo-second order plot for adsorption of Cu(II) ions on MSCB**

**Table 3**
**Parameters calculated from PFO and PSO kinetic model**

| Kinetic Model | Constant Values |
|---|---|
| Pseudo second order (PSO) | $q_{e\ (exp)}$(mg/g) = 48.36 |
| | $q_{e\ (exp)}$ (mg/g) = 52.91 |
| | $k_2$ (g $mg^{-1}$ $min^{-1}$) = 0.00045 |
| | $R^2$ = 0.9985 |
| Pseudo first order (PFO) | $q_{e\ (exp)}$(mg/g) = 48.36 |
| | $q_{e\ (cal)}$ (mg/g) = 38.12 |
| | $k_1$ ($min^{-1}$) = 0.0119 |
| | $R^2$ = 0.9764 |

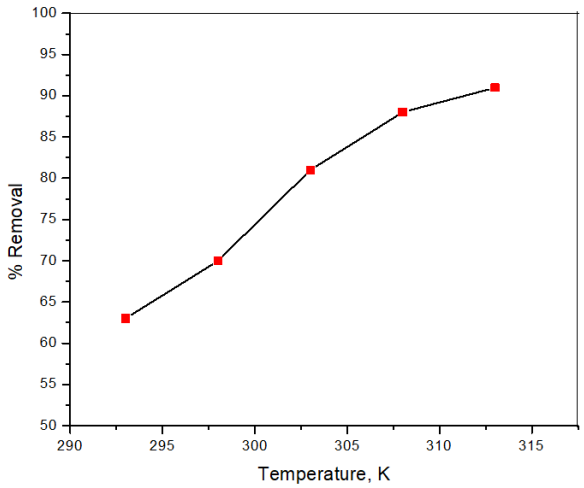


**Figure 7: Influence of temperature on % removal of Cu(II) at MSCB dose = 1.0 g/L, pH = 4.5 ± 0.1, [Cu(II)] = 20 mg/L and Contact time = 230 min**

**Table 4**
**Thermodynamic parameters for Cu(II) adsorption onto MSCB**

| Temp (K) | $E_a$ kJ $mole^{-1}$ | $\Delta H^{\#}$ kJ $mole^{-1}$ | $\Delta S^{\#}$ J $K^{-1}$ $mole^{-1}$ | $\Delta G^{\#}$ kJ $mole^{-1}$ | $K_c$ |
|---|---|---|---|---|---|
| 303 | 48.3 | 47.78 | 157.77 | - 2.03 | 6.38 |

Equations 9-11 were used to evaluate the thermodynamic activation parameters. Equation 9 provides the relationship between the equilibrium constant $K_c$ and standard Gibbs free energy (ΔG°) at any temperature T:

$$\Delta G° = -RT \ln K_C \quad (9)$$

Equation 10 provides the relationship between the entropy (ΔS°) and enthalpy (ΔH°) of adsorption with the standard free energy change (ΔG°), while equation 11 defines $K_c$:

$$lnK_c = -\left(\frac{\Delta G^o}{RT}\right) = -\left(\frac{\Delta H^o}{RT}\right) + \left(\frac{\Delta S^o}{R}\right) \quad (10)$$

$$K_C = \frac{C_a}{C_e} \quad (11)$$

In this context, the equilibrium concentration is denoted as $C_e$ while the amount of Cu(II) ions that are adsorbed at equilibrium is represented as $C_a$. The computed values of the various parameters have been summarized in table 4. The Cu(II) adsorption onto MSCB seems to exhibit an endothermic nature, as suggested by the positive value of ΔH°. The elevated ΔS° may stem from the interactions occurring at the interface between the solid and the solution. Furthermore, the negative ΔG° suggests that the Cu(II) adsorption onto MSCB occurs spontaneously.

**Desorption and Reusability of MSCB:** Desorption investigations aid in clarifying the adsorption process and the viability of recovering the used activated carbon. The research revealed that weak interactions like Van der Waals forces can be used to explain how an ion is attached to an adsorbent if the ions that are adsorbed on the solid surface, can be desorbed by water[40]. If the ion is desorbable by acidic or alkaline water, an ion exchange takes place during the adsorption process. The desorption percentages of $H_2O$, 0.1 M MaOH and 0.1 M HCl were determined to be 0.28%, 3.51% and 79.36% respectively.

This outcome was anticipated since the presence of acidic conditions allowed $H_3O^+$ ions to protonate the adsorbent surface, hence facilitating the desorption of positively charged Cu(II).

Moreover, a mechanism involving ion exchange was identified and it was found that HCl is an effective reagent for regenerating the Cu(II)-loaded MSCB. Afterwards, the impact of five successive adsorption-desorption runs on the Cu(II) adsorption by MSCB was investigated. The desorbed MSCB proved to be extremely efficient in readsorbing Cu(II), with the recycled Cu(II)- MSCB showing a slight decrease in adsorption capacity of approximately 7.2% by the fifth cycle. It may be inferred that the Cu(II)- MSCB can be employed multiple times without drastically reducing its adsorption capabilities.

## Conclusion

Current research examines Cu(II) ion adsorption on modified sugarcane bagasse (MSCB) in aqueous medium. For optimal adsorption of Cu(II) ions onto MSCB, a pH value of 4.5 was determined to be the most effective with an adsorption capacity of 62.11 mg/g. It also shows that the absorption of Cu(II) ions was fast until 110 minutes, after which it reached equilibrium at 230 minutes. The substantial pH dependence of Cu(II) adsorption on MSCB suggests a mechanism involving ion exchange.

The adsorption proceeds according to pseudo-second-order kinetics and the Langmuir isotherms provide a good fit for the equilibrium data. MSCB exhibits a remarkable capacity for regeneration. Thus, MSCB shows promise as a cost-effective and efficient adsorbent for adsorbing Cu(II) ions from water-based solutions.

## References

1. Abdel-Nasser A. and El-Hendawy A.A., Influence of HNO3 oxidation on the structure and adsorptive properties of corncob-based activated carbon, *Carbon*, **41**, 713-722 **(2003)**

2. Aguilar C., Garcıía R., Soto-Garrido G. and Arriagada R., Catalytic wet air oxidation of aqueous ammonia with activated carbon, *Applied Catalysis B: Environment and Energy*, **46**, 229-237 **(2003)**

3. Ali S.W., Waqar F., Malik M.A., Yasin T. and Muhammad B., Study on the synthesis of a macroporous ethylacrylate-divinylbenzene copolymer, its conversion into a bi-functional cation exchange resin and applications for extraction of toxic heavy metals from wastewater, *Journal of Applied Polymer Science*, **129**, 2234-2243 **(2013)**

4. Alsohaimi I.H., Alhumaimess M.S., Hassan H.M.A., Reda M., Aldawsari A.M., Chen Q. and Kariri M.A., Chitosan Polymer Functionalized-Activated Carbon/Montmorillonite Composite for the Potential Removal of Lead Ions from Wastewater, *Polymers*, **15(9)**, 2188 **(2023)**

5. Ani J.U., Akpomie K.G. and Okoro U.C., Potentials of activated carbon produced from biomass materials for sequestration of dyes, heavy metals and crude oil components from aqueous environment, *Applied Water Science*, **10**, 69 **(2020)**

6. Assi M.A., Hezmee M.N., Haron A.W., Sabri M.Y. and Rajion M.A., The detrimental effects of lead on human and animal health, *Veterinary World*, **9(6)**, 660-671 **(2016)**

7. Barka N., Abdennouri M., El Makhfouk M. and Qourzal S., Biosorption characteristics of cadmium and lead onto eco-friendly dried cactus (Opuntia ficus indica) cladodes, *Journal of Environmental Chemical Engineering*, **1**, 144-149 **(2013)**

8. Bhuiyan M.A.H., Parvez L., Islam M.A., Dampare S.B. and Suzuki S., Heavy metal pollution of coal mine-affected agricultural soils in the northern part of Bangladesh, *Journal of Hazardous Materials*, **173**, 384-392 **(2010)**

9. Boudrahem F., Aissani-Benissad F. and Soualah A., Adsorption of lead (II) from aqueous solution by using leaves of date trees as an adsorbent, *Journal of Chemical & Engineering Data*, **56**, 1804-1812 **(2011)**

10. Bouhamed F., Zouheir E. and Jalel B., Adsorptive removal of copper(II) from aqueous solutions on activated carbon prepared from Tunisian date stones: Equilibrium, kinetics and thermodynamics, *Taiwan Institute of Chemical Engineering*, **43**, 741-749 **(2012)**

11. Cheng H. and Hu Y., Lead (Pb) isotopic fingerprinting and its applications in lead pollution studies in China: a review, *Environmental Pollution*, **158**, 1134-1146 **(2010)**

12. Darweesh M.A., Elgendy M.Y., Ayad M.I., Ahmed A.M., Kamel Elsayed N.M. and Hammad W.A., Adsorption isotherm, kinetic and optimization studies for copper (II) removal from aqueous solutions by banana leaves and derived activated carbon, *South African Journal of Chemical Engineering*, **40**, 10-20 **(2022)**

13. Das S., Sultana K.W., Ndhlala A.R., Mondal M. and Chandra I., Heavy Metal Pollution in the Environment and Its Impact on Health: Exploring Green Technology for Remediation, *Environmental Health Insights*, **17**, 11786302231201259 **(2023)**

14. Demiral H. and Güngor C., Adsorption of copper(II) from aqueous solutions on activated carbon prepared from grape bagasse, *Journal of Cleaner Production*, **124**, 103-113 **(2016)**

15. Díaz-Díez M.A., Gómez-Serrano V. and Fernández González C., Porous texture of activated carbons prepared by phosphoric acid activation of woods, *Applied Surface Science*, **238**, 309-313 **(2004)**

16. Freundlich H., Adsorption in solution, *Physical Chemistry Society*, **40**, 1361-1368 **(1906)**

17. Futalan C.C., Diana E., Edang M.F.A., Padilla J.M., Cenia M.C. and Alfeche D.M., Adsorption of Lead from Aqueous Solution Using Activated Carbon Derived from Rice Husk Modified with Lemon Juice, *Sustainability*, **15(22)**, 15955 **(2023)**

18. Goswami M.K., Srivastava A., Dohare R.K., Tiwari A.K. and Srivastava A., Recent Advances on Conducting Polymer Based Magnetic Nanosorbents for Dyes and Heavy Metal removal: Fabrication, Applications and Perspective, *Environmental Science Pollution and Research*, **30**, 73031-73060 **(2023)**

19. Gu S., Wang L., Mao X., Yang L. and Wang C., Selective Adsorption of Pb(II) from Aqueous Solution by Triethylenetetramine-Grafted Polyacrylamide/Vermiculite, *Materials*, **11(4)**, 514 **(2018)**

20. Hama Aziz K.H., Mustafa F.S., Omer K.M., Hama S., Hamarawf R.F. and Rahman K.O., Heavy metal pollution in the aquatic environment: efficient and low-cost removal approaches to eliminate their toxicity: a review, *RSC Advances*, **13(26)**, 17595-17610 **(2023)**

21. Huang K. and Zhu H., Removal of $Pb^{2+}$ from aqueous solution by adsorption on chemically modified muskmelon peel, *Environmental Science and Pollution Research*, **20**, 4424-4434 **(2013)**

22. Iqbal M., Saeed A. and Zafar S.I., FTIR spectrophotometry, kinetics and adsorption isotherms modeling, ion exchange and EDX analysis for understanding the mechanism of $Cd^{2+}$ and $Pb^{2+}$ removal by mango peel waste, *Journal of Hazardous Materials*, **164**, 161-171 **(2009)**

23. Iqbal M., Saeed A. and Kalim I., Characterization of Adsorptive Capacity and Investigation of Mechanism of $Cu^{2+}$, $Ni^{2+}$ and $Zn^{2+}$ Adsorption on Mango Peel Waste from Constituted Metal Solution and Genuine Electroplating Effluent, *Separation Science and Technology*, **44**, 3770-3791 **(2009)**

24. Kalavathy M.H., Karthikeyan T. and Rajgopal S., Kinetic and isotherm studies of Cu(II) adsorption onto H3PO4-activated rubber wood sawdust, *Journal of Colloid and Interface Science*, **292**, 354-362 **(2005)**

25. Kapil S., Sharma V. and Kumar T., Characterization of Bacillus tequilensis A1C1: A Novel Bio-reservoir of D-serine, *Res. J. Biotech.*, **18(2)**, 8-14 **(2023)**

26. Kumar A. and Jena H.M., Preparation and Characterization of High Surface Area Activated Carbon from Fox Nut (Euryale ferox) Shell by Chemical Activation with H3PO4, *Results in Physics*, **6**, 651-658 **(2016)**

27. Kumar G.P., Malla K.A., Yerra B. and Rao K.S., Removal of Cu(II) using three low-cost adsorbents and prediction of adsorption using artificial neural networks, *Applied Water Science*, **9**, 44 **(2019)**

28. Langmuir I., The adsorption of gases on plane surfaces of glass, mica and platinum, *Journal of American Chemical Society*, **40**, 1361-1403 **(1918)**

29. Li Y.H., Di Z.C., Ding J., Wu D.H., Luan Z.K. and Zhu Y.Q., Adsorption thermodynamic, kinetic and desorption studies of Pb2+ on carbon nanotubes, *Water Research*, **39**, 605–609 **(2005)**

30. Mitra S., Chakraborty A.J., Tareq A.M., Emran T.B., Nainu F., Khusro A., Idris A.M., Khandaker M.U., Osman H., Alhumaydhi F.A. and Simal-Gandara J., Impact of heavy metals on the environment and human health: Novel therapeutic insights to counter the toxicity, *Journal of King Saud University Science*, **34**, 101865 **(2022)**

31. Moore R.Z., Wilson V., Hou A. and Meng G., Source of lead pollution, its influence on public health and the countermeasures. International Journal of Health, *Animal Science & Food Safety*, **2**, 18-31 **(2015)**

32. Moreno-Castilla C., Lopez-Ramon M.V. and Carrasco-Marın F., Changes in surface chemistry of activated carbons by wet oxidation, *Carbon*, **38**, 1995–2001 **(2000)**

33. Moreno-Pirajan J.C. and Giraldo L., Adsorption of copper from aqueous solution by activated carbons obtained by pyrolysis of cassava peel, *Journal of Analytical and Applied Pyrolysis*, **87**, 188-193 **(2010)**

34. Muttil N., Jagadeesan S., Chanda A., Duke M. and Singh S.K., Production, Types and Applications of Activated Carbon Derived from Waste Tyres: An Overview, *Applied Sciences*, **13**, 257 **(2023)**

35. Namasivayam C. and Kavitha D., IR, XRD and SEM studies on the mechanism of adsorption of dyes and phenols by coir pith carbon from aqueous phase, *Microchemical Journal*, **82**, 43-48 **(2006)**

36. Namasivayam C. and Yamuna R.T., Removal of Rhodamine-B by biogas waste slurry from aqueous solutions, *Water Air & Soil Pollution*, **65**, 101-109 **(1992)**

37. Odumbe E., Murunga S. and Ndiiri J., Heavy Metals in Wastewater Effluent: Causes, Effects and Removal Technologies, *Intech Open*, doi: 10.5772/intechopen.1001452 **(2023)**

38. Rengaraj S., Joo C.K., Kim Y. and Yi J., Kinetics of removal of chromium from water and electronic process wastewater by ion exchange resins 1200H, 1500H and IRN97H, *Journal of Hazardous Mater*, **102**, 257-275 **(2003)**

39. Ryu Z., Zheng J., Wang M. and Zhang B., Characterization of pore size distributions on carbonaceous adsorbents by DFT, *Carbon*, **37**, 1257-1264 **(1999)**

40. Schneider R.M., Cavalin C.F., Barros M. and Tavares C.R.G., Adsorption of chromium ions in activated carbon, *Chemical Engineering Journal*, **132**, 355-362 **(2007)**

41. Singh V., Ahmed G. and Vedika S., Toxic heavy metal ions contamination in water and their sustainable reduction by eco-friendly methods: isotherms, thermodynamics and kinetics study, *Scientific Reports*, **14**, 7595 **(2024)**

42. Wang B., Lan J., Bo C., Gong B. and Ou J., Adsorption of heavy metal onto biomass-derived activated carbon: review, *RSC Advances*, **13(7)**, 4275-4302 **(2023)**

43. Wani A.L., Ara A. and Usmani J.A., Lead toxicity: a review, *Interdisciplinary Toxicology*, **8(2)**, 55-64 **(2015)**

44. Weber T.W. and Chakkravorti R.K., Pore and solid diffusion models for fixed bed adsorbers, *American Institute of Chemical Engineering Journal*, **20**, 228 **(1974)**.

(Received 07th January 2025, accepted 11th March 2025)